Efficient energy transfer and photoluminescent characteristics in $SrAl_{12}O_{19}:Eu^{2+},Cr^{3+}$ nano-rods

2007 Nanotechnology 18 445707

(http://iopscience.iop.org/0957-4484/18/44/445707)

IOP PUBLISHING NANOTECHNOLOGY
Nanotechnology **18** (2007) 445707 (5pp) doi:10.1088/0957-4484/18/44/445707

Efficient energy transfer and photoluminescent characteristics in $SrAl_{12}O_{19}:Eu^{2+}$, Cr^{3+} nano-rods

Ruixia Zhong[1,2], **Jiahua Zhang**[1,4], **Xia Zhang**[1], **Shaozhe Lu**[1] and **Xiao-jun Wang**[1,3]

[1] Key Laboratory of Excited State Processes, Changchun Institute of Optics, Fine Mechanics and Physics, Chinese Academy of Sciences, 16 Eastern South Lake Road, Changchun 130033, People's Republic of China
[2] Graduate School of Chinese Academy of Sciences, Beijing 100039, People's Republic of China
[3] Department of Physics, Georgia Southern University, Statesboro, GA 30460, USA

E-mail: zhangjh@ciomp.ac.cn

Received 27 June 2007, in final form 27 August 2007
Published 10 October 2007
Online at stacks.iop.org/Nano/18/445707

Abstract
Cr^{3+} singly doped and Eu^{2+}, Cr^{3+} co-doped $SrAl_{12}O_{19}$ nano-rods with different diameters have been prepared by a combustion method. A new emission band of Cr^{3+} centered at 704 nm on the low energy side of the R-line at 688 nm originating from the ^2E–$^4A_2$ transition of Cr^{3+} is observed. This band enhances with decreasing diameter of the nano-rods, implying its origin in the Cr^{3+} ions on the surface of the nano-rods. Photoluminescence study and fluorescence lifetime measurements demonstrate efficient energy transfer from Eu^{2+} to Cr^{3+} in $SrAl_{12}O_{19}$ nano-rods in comparison with the corresponding bulk materials. This result is attributed to a large spectral overlap between the Eu^{2+} emission band and the $^4A_2$–$^4T_1$ (F) absorption band of Cr^{3+} on the surface of the nano-rods.

1. Introduction

Over the past several years, there has been an ongoing search for nano-sized phosphors with superior performance characteristics over their micrometer counterparts. This research has been stimulated by the fact that significant changes in the optical properties have been observed with decreasing particle size [1, 2]. Meanwhile, a greater degree of disorder on the surface in the nano-phase significantly influences its vibrational characteristics. The surface phonon modes are intensified due to the higher number of surface atoms. In this case, the electron–phonon coupling can be significantly strong in nano-materials [3, 4].

Currently, the search for a new solid-state tunable laser in the visible and near infrared spectral region has generated interest in the study of different types of materials doped with rare-earth or transition-metal ions [5–8]. The Cr^{3+} ion is a good candidate for a solid-state laser to obtain sharp or broad spectral lasers depending on the symmetry of the states involved and on the dynamic of the environment surrounding the active ions in the crystal [9, 10]. Meanwhile, the Cr^{3+} ion with red emission is one of the most used activators for luminescent materials [11]. As is known, strontium aluminates doped with rare-earth metal ions have attracted much attention for their excellent properties such as high quantum efficiency and good stability. In particular, $SrAl_{12}O_{19}:Eu^{2+}$ shows a bright blue emission at 400 nm with high quantum efficiency of 90% [12]. In our previous work, the energy transfer from Eu^{2+} to Cr^{3+} has been found in the system of $Sr_4Al_{14}O_{25}:Eu^{2+}$, Cr^{3+} [13, 14].

In this paper, we report to our knowledge for the first time on the synthesis and photoluminescent characteristics of $SrAl_{12}O_{19}:Eu^{2+}$, Cr^{3+} nano-rods. The energy transfer from Eu^{2+} to Cr^{3+} and the deep red emission of Cr^{3+} have been studied in both the bulk material and nano-rods. It is found that a broad emission band appears at 704 nm in the $SrAl_{12}O_{19}$ nano-rods containing Cr^{3+}. It is observed that the energy

[4] Author to whom any correspondence should be addressed.

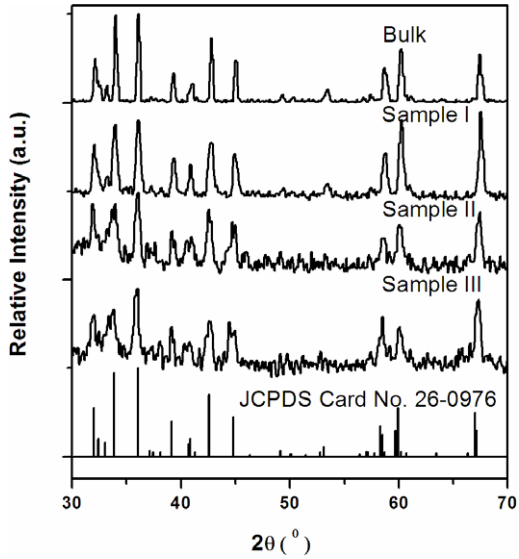

Figure 1. The x-ray powder diffraction patterns (XRD) of bulk-$SrAl_{12}O_{19}$:1% Cr^{3+}, samples I, II and III.

transfer from Eu^{2+} to Cr^{3+} is more efficient in $SrAl_{12}O_{19}$ nano-rods than in the bulk material.

2. Experiments

$SrAl_{12}O_{19}$:Eu^{2+}, Cr^{3+} phosphor nano-rods have been prepared by the combustion method. In a cylindrical container, a stoichiometric composition of aluminum nitrate ($Al(NO_3)_3$), strontium nitrate ($Sr(NO_3)_3$), europium nitrate ($Eu(NO_3)_3$) and chromium nitrate ($Cr(NO_3)_3$) is dissolved in a minimum amount of distilled water together with an amount of urea. Initially, the solution boils and undergoes dehydration, followed by decomposition for all the nitrates with the evolution of large amounts of gases. Then, spontaneous ignition for urea occurs and it undergoes smouldering combustion with enormous swelling, producing white foamy and voluminous $SrAl_{12}O_{19}$:Eu^{2+}, Cr^{3+}. The combustion reaction can be described as follows:

$$Sr(NO_3)_2 + 12Al(NO_3)_3 + \tfrac{1}{3}95NH_2CONH_2 \rightarrow SrAl_{12}O_{19} + \tfrac{1}{3}152N_2 \uparrow + \tfrac{1}{3}95CO_2 \uparrow + \tfrac{1}{3}190H_2O.$$

The whole process is over within less than 3 min. The Bulk $SrAl_{12}O_{19}$:Eu^{2+}, Cr^{3+} phosphors have been also synthesized at 1400 °C by the usual solid-state reaction technique under a weak reductive atmosphere of active carbon for comparison, and boric acid is added to the mixture as flux. All starting materials are of analytical purity.

The emission and excitation spectra are measured with a Hitachi F-4500 Spectra-fluorometer. The crystalline structure of the sample is investigated by x-ray diffraction (XRD) using a Siemens D-500 equipment with a Cu target radiation source. Scanning electron micrographs (SEMs) are taken on S-4800 (Hitachi Company) electron microscopes. In lifetime measurements, the fourth (266 nm) harmonic of a Nd–YAG laser (Spectra-Physics, GCR 130) is used as an excitation source, and the signal is detected with a Tektronix digital oscilloscope model (TDS 3052).

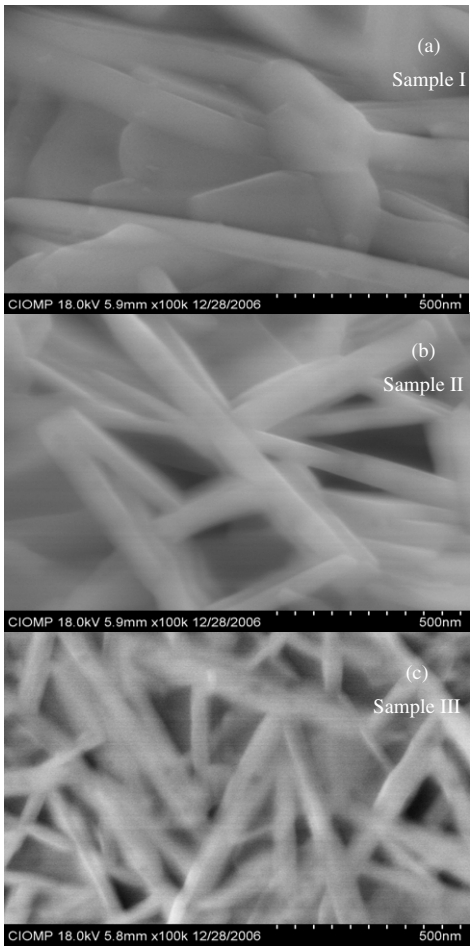

Figure 2. The SEMs of samples I, II and III.

3. Results and discussion

The $SrAl_{12}O_{19}$:1% Cr^{3+} nano-rods with different diameters were prepared by a combustion method. The samples with mean diameters 150, 70 and 50 nm are named sample I, sample II and sample III, respectively. The x-ray powder diffraction patterns (XRD) of bulk-$SrAl_{12}O_{19}$:1% Cr^{3+}, samples I, II and III and the scanning electron micrographs (SEMs) of samples I, II and III are shown in figures 1 and 2, respectively. Samples I, II and III are the nano-rods with average length about 1 μm. The XRD patterns of all the synthesized samples have matched with JCPDS (26-0976), which can be indexed on the space group of $P6_3/mmc$ for hexagonal $SrAl_{12}O_{19}$ with the magnetoplumbite-type structure.

The emission (dash–dot lines; $\lambda_{ex} = 588$ nm) and excitation (solid lines, $\lambda_{em} = 688$ nm; short dot lines, $\lambda_{em} = 704$ nm) spectra of a $SrAl_{12}O_{19}$:1% Cr^{3+} bulk material and the three nano-rod samples I, II and III are shown in figures 3(a)–(d), respectively. In the emission spectra of both bulk and nano-materials, there appears an emission line at 688 nm, which is the well known R-line originating from the ^2E–$^4A_2$ transition of Cr^{3+}. Meanwhile, a sideband centered at 704 nm is observed in the nano-rods and this band grows relative to the 688 nm R-line with decreasing diameters of the nano-rods. The emission line at 694 nm in the emission spectra of the nano-

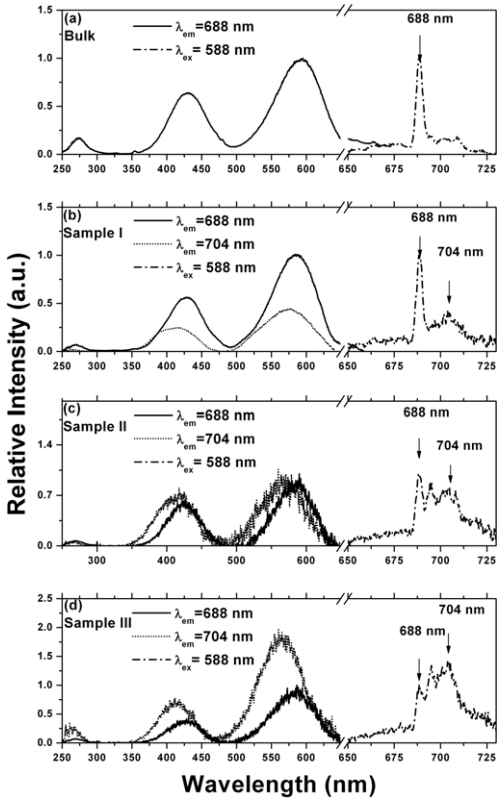

Figure 3. Emission (dash–dot lines; $\lambda_{ex} = 588$ nm) and excitation (solid lines, $\lambda_{em} = 688$ nm; short dot lines, $\lambda_{em} = 704$ nm) spectra of a $SrAl_{12}O_{19}$:1% Cr^{3+} bulk material and the nano-rod samples I, II and III.

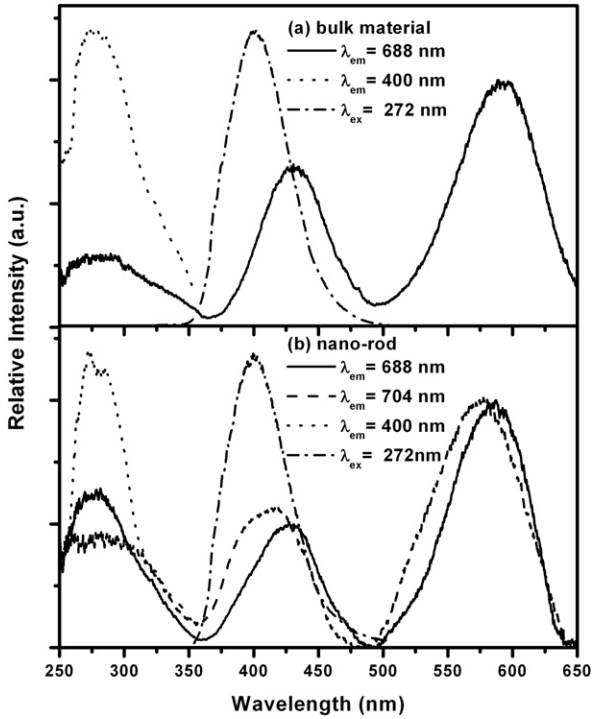

Figure 4. Comparison of the emission (dash–dot lines, $\lambda_{ex} = 272$ nm) and excitation spectra (dot lines, $\lambda_{em} = 400$ nm) of Eu^{2+} with excitation spectra (solid lines, $\lambda_{em} = 688$ nm; dash lines, $\lambda_{em} = 704$ nm) of Cr^{3+} in bulk (a) and nano-rod (b) $SrAl_{12}O_{19}$:1% Eu^{2+}, 1% Cr^{3+}.

rods originates from the ^2E–$^4A_2$ transition of Cr^{3+} in the Al_2O_3 phase, which is not of interest in this work. In the excitation spectra monitoring the 688 nm R-lines of both the nano-rods and bulk material, there appear two major bands peaking at 427 and 588 nm, which originate from $^4A_2$–$^4T_1$ (F) and $^4A_2$–$^4T_2$ (F) transitions of Cr^{3+}, respectively. One can also find that the two excitation bands in the excitation spectra monitoring the 704 nm band in the nano-rods peak at 410 nm and 565 nm, respectively. The weak $^4A_2$–$^4T_1$ (P) transition appears in the ultraviolet region. This indicates that the Cr^{3+} ions responsible for the 704 nm band are located in an environment which is different from that which the Cr^{3+} ions responsible for the 688 nm R-lines are located at. In view of the enhancement of the 704 nm band with reducing size of the nano rods, it is speculated that this band is responsible for the Cr^{3+} ions on the surface of the nano-rods. Two possible origins of the 704 nm band are considered in this work. One is the ^2E–$^4A_2$ transition of Cr^{3+} on the surface of the nano-rods. The disordered environments on the surface of the nano-rods may broaden the ^2E–$^4A_2$ emission lines. The other origin is the phonon sideband of the ^2E–$^4A_2$ transition of Cr^{3+} on the surface of the nano-rods. From the theoretical results of Tamura *et al* [15], the modes of the phonons can be classified into two types: the inner modes having high eigenfrequencies and the surface modes having low eigenfrequencies. The surface-to-volume ratio increases rapidly in nanoparticles. Thus, the surface modes having low eigenfrequencies make more contributions to the phonon sidebands. As is known, the diameter of the electronic wavefunction of ^2E state of Cr^{3+} is so small that the size confinement effect does not work. However, for the wavefunction of a long acoustic wave, the size confinement effect is valid: the confinement of the vibration excitations produces a greatly enhanced interaction between the ion electron states and the vibrational modes [16]. Thus, the phonon sideband may become extremely strong in the nano-rods. If the 704 nm band is a phonon sideband, the zero-phonon line of the sideband has not been detected yet even at 77 K. This may be a result of the zero-phonon line being hidden in the 688 nm line or being too weak to be observed because of strong electron–phonon coupling.

The Eu^{2+} and Cr^{3+} co-doped nano-rods have been prepared. The mean diameters of the co-doped nano-rods are 70 nm. Figure 4 presents the comparison of emission spectra of Eu^{2+} with excitation spectra of Cr^{3+} in bulk (a) and nano-rod (b) $SrAl_{12}O_{19}$:1% Eu^{2+}, 1% Cr^{3+}. It is clearly demonstrated that there exists a spectral overlap between the emission band of Eu^{2+} peaking around 400 nm and the $^4A_2$–$^4T_1$ (F) excitation band of Cr^{3+} peaking at 427 nm. A band originating from the f–d transition of Eu^{2+} is observed in the spectral range of 250–350 nm in the excitation spectra monitoring Cr^{3+} emissions, indicating the performance of energy transfer from Eu^{2+} to Cr^{3+} in $SrAl_{12}O_{19}$. Moreover, one can observe that the excitation band at 410 nm for the 704 nm emission band in $SrAl_{12}O_{19}$:1% Eu^{2+}, 1% Cr^{3+} nano-rods overlaps largely with the emission band of Eu^{2+} at 400 nm, predicting more efficient energy transfer between Eu^{2+} and Cr^{3+} in $SrAl_{12}O_{19}$ nano-rods than bulk material.

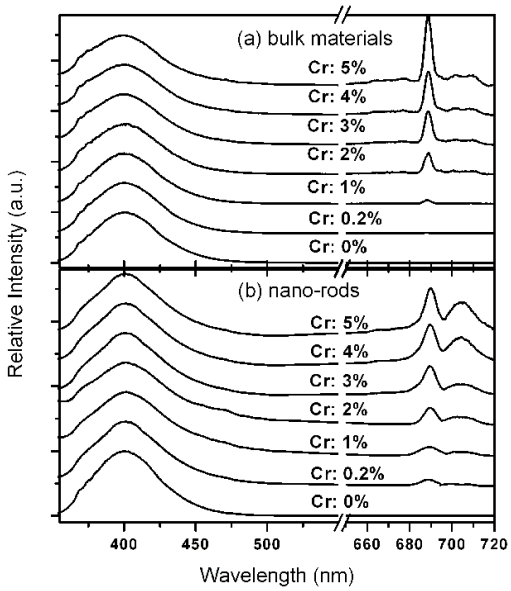

Figure 5. Emission spectra of $SrAl_{12}O_{19}$: 1% Eu^{2+}, x% Cr^{3+} ($x = 0$, 0.2, 1, 2, 3, 4 and 5; $\lambda_{ex} = 300$ nm): (a) bulk materials; (b) nano-rods.

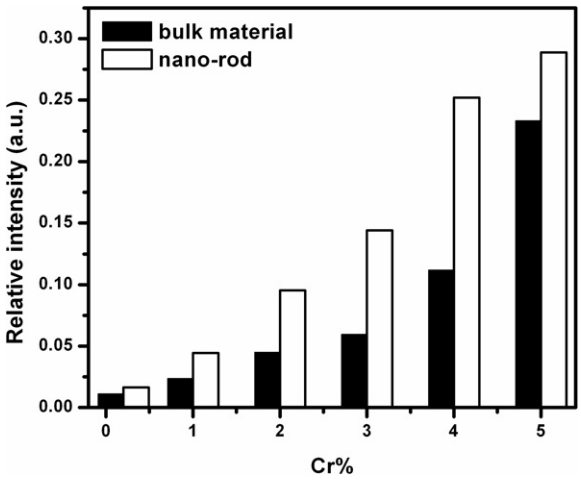

Figure 6. Dependence of the ratio for the red emission to the blue one on the Cr^{3+} concentration.

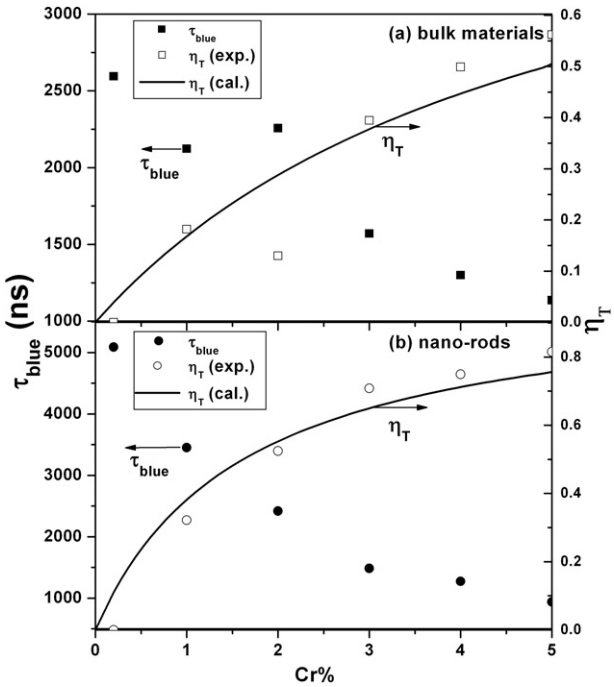

Figure 7. Dependence of the energy transfer efficiency (η_T) and lifetime of Eu^{2+} ions on the Cr^{3+} concentration.

The emission spectra of $SrAl_{12}O_{19}$:1% Eu^{2+}, x% Cr^{3+} ($x = 0$, 0.2, 1, 2, 3, 4 and 5) for the bulk materials and the nano-rods are shown in figures 5(a) and (b), respectively. The intensities of 400 nm emission are normalized. For the bulk materials in figure 5(a), the Cr^{3+} emission at 688 nm increases following the increasing Cr^{3+} concentration. For the nano-rods in figure 5(b), both the R-line at 688 nm and the 704 nm band enhance with increasing Cr^{3+} concentration. The excitation at 300 nm can only directly excite Eu^{2+} not Cr^{3+}, because there is no absorption at 300 nm for Cr^{3+}, as shown in figure 3. The strong red emission of Cr^{3+} also in $SrAl_{12}O_{19}$:1% Eu^{2+}, x% Cr^{3+} nano-rods under 300 nm excitation is therefore the evidence of energy transfer between Eu^{2+} and Cr^{3+}. According to the emission spectra shown in figure 5, the intensity ratios of the red emission of Cr^{3+} to the blue emission of Eu^{2+} are plotted as a function of Cr^{3+} concentrations, as shown in figure 6. The ratio grows with increasing Cr^{3+} concentration for both the bulk material and the nano-rods. The ratio is found to be high for the nano-rods compared to the bulk material under the same concentration of Cr^{3+}. This indicates an efficient energy transfer from Eu^{2+} to Cr^{3+} in the nano-rods.

In order to analyze the energy transfer efficiency as a function of Cr^{3+} concentration, the lifetimes of 400 nm (τ_{blue}) emissions in both bulk and nano-rods $SrAl_{12}O_{19}$:1% Eu^{2+}, x% Cr^{3+} ($x = 0.2$, 1, 2, 3, 4 and 5) are measured and shown in figures 7(a) and (b), respectively. All the decays can be described as a single exponential function. The lifetimes of Eu^{2+} reduce with increasing Cr^{3+} concentration because of the energy transfer from Eu^{2+} to Cr^{3+}. The reduction of the lifetimes of Eu^{2+} is larger in the nano-rods than in bulk, arresting the efficient energy transfer in the nano-rods. The energy transfer efficiency (η_T) as a function of Cr^{3+} concentration is investigated. According to the definition suggested by Paulose *et al* [17], η_T can be expressed by

$$\eta_T = 1 - \frac{\tau_{blue}}{\tau_{blue,0}}, \tag{1}$$

where $\tau_{blue,0}$ is the intrinsic decay lifetime of Eu^{2+} without Cr^{3+} co-doping.

As is known, the macroscopic energy transfer rate W_{Eu-Cr} as a function of Cr^{3+} concentration can be evaluated from the lifetime measurement since $W_{Eu-Cr} = 1/\tau_{blue} - 1/\tau_{blue,0}$. The single exponential decay of the blue emission for various Cr^{3+} concentrations is the reflection of efficient energy diffusion between Eu^{2+} rather than transfer to Cr^{3+}. The energy transfer rate between Eu^{2+} and Cr^{3+} is considered to be

a linear relationship with the Cr^{3+} concentration, described as a function of $W_{Eu-Cr} = aC_{Cr}$, where C_{Cr} is the Cr^{3+} concentration; a is the constant for the energy transfer rate.

Using equation (1) and the measured lifetimes, the energy transfer efficiencies of the bulk materials and the nano-rods have been obtained and shown in figures 7(a) and (b), respectively. The calculated curves in figure 7 are drafted according to the relationship between the energy transfer rate (W_{Eu-Cr}) and energy transfer efficiency (η_T) expressed by

$$\eta_T = 1 - \frac{1}{a\tau_{blue,0}C_{Cr} + 1}. \quad (2)$$

The value of a is 8×10^6 (s^{-1} mol^{-1}) for the bulk materials and 1.2×10^7 for the nano-rods, which are obtained by fitting the experimental data using equation (2). The calculated curves perfectly agree with the experimental data for both the bulk material and the nano-rods. With the increasing Cr^{3+} concentration, the transfer efficiency in the nano-rods grows faster than that in the bulk materials.

The lifetimes of 688 and 704 nm in the nano-rods with 1% Eu^{2+} and 0.2% Cr^{3+} co-doped are 2.56 and 2.45 ms, respectively, while they reduce to 1.7 and 1.9 ms in the nano-rods with 1% Eu^{2+} and 5% Cr^{3+} co-doped. The different lifetimes for 688 and 704 nm indicate that the zero-phonon line of 704 nm is not the emission line at 688 nm as in the foregoing discussion. The reductions of the lifetimes of 688 and 704 nm are small, indicating the slow energy diffusion between Cr^{3+} ions. Thus, the energy transfer between Cr^{3+} ions can be ignored.

As in the discussion above, the Cr^{3+} on the surface of the nano-rods gives the strong emission band at 704 nm. The excitation spectrum of 704 nm emission moves to the shorter wavelength, which has more overlaps with the Eu^{2+} emission, leading to the efficient energy transfer from Eu^{2+} to Cr^{3+} in the nano-rods.

4. Conclusions

In summary, a deep red emission band centered at 704 nm appears in the nano-rod containing Cr^{3+} ions and this band grows following the decreasing diameters of the nano-rods. It is speculated that this band is responsible for the Cr^{3+} ions on the surface of the nano-rods. The origin of the 704 nm band may be the ^2E–$^4A_2$ transition or its phonon sideband of Cr^{3+} on the surface of the nano-rods. The energy transfer efficiency in the nano-rod is high compared to the bulk material because the absorption band of $^4A_2$–$^4T_1$ (F) transition at 410 nm of the Cr^{3+} on the surface of the nano-rod overlaps largely with the emission band of Eu^{2+} at 400 nm in Eu^{2+} and Cr^{3+} co-doped $SrAl_{12}O_{19}$ nano-rods. The efficient transfer in the nano-rods leads to the following results: (1) the strong absorption band of Eu^{2+} f–d transition appears in the excitation spectra of Cr^{3+} emission for the nano-rods; (2) the ratio of the red emission of Cr^{3+} to the blue of Eu^{2+} in the nano-rods is large and increases rapidly following the increasing of Cr^{3+} concentrations when only Eu^{2+} is optically excited. Thus, the nano-material of $SrAl_{12}O_{19}$:Eu^{2+}, Cr^{3+} may be used as a promising material for a solid-state tunable laser in the visible and near infrared spectral region because of the broad emission band originating from the Cr^{3+} ions on the surface and the efficient energy transfer.

Acknowledgments

This work is financially supported by MOST of China (2006CB601104, 2006AA03A138), and the National Nature Science Foundation of China (10574128, 10504031).

References

[1] Williams D K, Yuan H and Tissue B M 1999 *J. Lumin.* **83/84** 297
[2] Sun X H, Lam S, Sham T K, Heigl F, Jürgensen A and Wong N B 2005 *J. Phys. Chem.* B **109** 3120
[3] Lee J D 2006 *J. Chem. Phys.* **124** 194706
[4] Hasan Z, Dardona S and Konjhodzic A 2005 *J. Chem. Phys.* **123** 224715
[5] Nevado R, Cusso F, Lifante G, Caccavale F, Sada C and Segato F 2000 *J. Appl. Phys.* **88** 6183
[6] Jaque D, Capmany J, García Solé J, Brenier A and Boulon G 2000 *Appl. Phys.* B **70** 11
[7] Montoya E, Capmany J, Bausa L E, Kellner T, Diening A and Haber G 1999 *Appl. Phys. Lett.* **74** 3113
[8] Di Paolo R E, Cantelar E, Pernas P L, Lifante G and Cusso F 2001 *Appl. Phys. Lett.* **79** 4088
[9] Qui Y 1993 *J. Phys.: Condens. Matter* **5** 2041
[10] Kaminskii A A 1996 *Crystalline Lasers: Physical Processes and Operating Schemes* (Boca Raton, FL: CRC Press)
[11] Geusic J E, Marcos H M and Van Uitert L G 1964 *Appl. Phys. Lett.* **4** 182
[12] Blasse G and Bril A 1968 *Philips Res. Rep.* **23** 201
[13] Zhong R X, Zhang J H, Zhang X, Lu S Z and Wang X J 2006 *J. Lumin.* **119/120** 327
[14] Zhong R X, Zhang J H, Zhang X, Lu S Z and Wang X J 2006 *Appl. Phys. Lett.* **88** 201916
[15] Tamura A and Ichinokawa T 1983 *J. Phys. C: Solid State Phys.* **16** 4779
[16] Yang H, Hong K S, Feofilov S P, Tissue B M, Meltzer R S and Dennis W M 1999 *J. Lumin.* **83** 139
[17] Paulose P I, Jose G, Thomas V, Unnikrishnan N V and Warrier M K R 2003 *J. Phys. Chem. Solids* **64** 841